

Calorimetric study of carbon partitioning from martensite into austenite steel

Emmanuel De Moor,^{1,2} Cecilia Föjer,³ Jan Penning,² Amy J. Clarke,⁴ and John G. Speer¹

¹*Advanced Steel Processing and Products Research Center, Colorado School of Mines, Golden, Colorado 80401, USA*

²*Department of Materials Science and Engineering, Ghent University, Technologiepark 903, B-9052 Zwijnaarde, Belgium*

³*ArcelorMittal Research Industry Gent, OCAS NV, ArcelorMittal, J. Kennedylaan 3, B-9060 Zelzate, Belgium*

⁴*Materials Science and Technology Division, Los Alamos National Laboratory, Mail Stop G770, Los Alamos, New Mexico 87545, USA*

(Received 6 May 2010; revised manuscript received 28 July 2010; published 27 September 2010)

Quenching and partitioning (Q&P) has been developed as a novel steel heat treatment to produce advanced high-strength microstructures consisting of a martensitic matrix containing significant amounts of retained austenite. Austenite stabilization is hypothesized to result from decarburization of the martensite and transport into the austenite. Differential scanning calorimetry was employed to study Q&P microstructures. Two exothermic events were observed when heating a Q&P sample from room temperature to 600 °C. An activation energy suggesting a mechanism controlled by carbon diffusion in bcc iron is obtained for the first peak which is believed to be associated with carbon partitioning. The second peak is believed to be associated with austenite decomposition.

DOI: 10.1103/PhysRevB.82.104210

PACS number(s): 64.70.kd, 66.30.-h, 81.05.Bx, 07.20.Fw

Quenching and partitioning (Q&P) is receiving increased attention as a new way to produce high-strength microstructures consisting of a martensitic matrix containing significant amounts of carbon-stabilized retained austenite.¹ The process consists of a two-step heat treatment. After soaking above the A_{c3} temperature or in the intercritical region, the steel is quenched to a predetermined temperature in the M_s – M_f range to produce a partially martensitic, partially austenitic microstructure. The second, so-called partitioning step, aims at carbon enrichment of the austenite by carbon depletion of the martensite and carbon transport to the austenite. Thus, carbon-stabilized austenite is retained in the microstructure after final quenching to room temperature. Alloying with carbide inhibiting elements is believed helpful to retard some competing reactions that may decrease the potential level of carbon enrichment of austenite. Promising mechanical properties have been reported.^{2,3} Some fundamental aspects of the heat treatment are not fully understood, however.

Unlike high-temperature diffusional transformations accompanied by carbon partitioning, carbon partitioning after low-temperature martensitic transformation has received limited attention. This may be related to the fact that quenching is usually carried out all the way to room temperature resulting in nearly complete martensite formation in many steels, although significant fractions of retained austenite are also possible. Subsequent tempering heat treatments following quenching result in a variety of reactions, including formation of transition carbides or cementite and decomposition of retained austenite. In contrast to conventional quenching and tempering, the Q&P concept introduced a procedure to intentionally enhance the volume fraction of austenite that can be stabilized using carbon present in the martensite at the quenching temperature. Although significant retained austenite fractions have been measured following Q&P processing,^{2,4} the process of carbon partitioning from martensite into austenite is difficult to observe directly. In addition, another mechanism (bainite formation) exists that also leads to carbon-stabilized retained austenite, although it has been shown that the austenite volume fractions measured after Q&P heat treating cannot be solely attributed to the

bainite reaction and thus partitioning of carbon from martensite into austenite must be contributing to austenite stabilization.⁵

In the present contribution, Q&P microstructures are developed by heat treatment and selected conditions are analyzed using differential scanning calorimetry (DSC). DSC has been shown to be a very sensitive technique for the study of reactions.^{6,7} In steels, DSC is particularly useful for those reactions associated with limited or no dimensional changes such as carbon clustering where dilatometry is less effective. DSC has been applied in calorimetric studies of martensite tempering, for example.⁷

A 0.20C-1.63Mn-1.63Si steel composition was used. The steel was received as cold rolled sheets. Coupons 30 mm × 30 mm were heat treated using salt baths. Soaking was done at 850 °C for 150 s resulting in full austenitization. The samples were then quenched to a temperature of 240 °C and held for 3 s. This temperature was calculated to maximize austenite fraction according to the method proposed by Speer *et al.*^{1,8} The partitioning was done at partitioning temperatures (PT) of 350, 400, and 450 °C for times ranging from 10 to 300 s followed by water quenching (WQ). Retained austenite volume fractions were determined by magnetic saturation measurements⁹ using a LakeShore 480 fluxmeter. X-ray diffraction (XRD) analysis was carried out on selected samples for retained austenite volume fraction and carbon-content determination, using a Siemens Kristalloflex D5000 diffractometer using Mo $K\alpha$ radiation operating at 50 kV and 50 mA. Samples were scanned over a 2θ range from 15° to 55°, at a step size of 0.02°, with a dwell time of 1 s. The background radiation and $K\alpha_2$ contributions to intensity were stripped. The retained austenite volume fraction was determined with the direct comparison method¹⁰ using the integrated intensity of the (200)_a, (211)_a, (220)_a, and (311)_a peaks. The carbon content was determined according to Cullity.¹⁰ The average carbon content was obtained using the positions of both austenite peaks. It should be noted that a significant difference exists between the retained austenite fractions measured by both techniques which has been reported previously in a blind round robin test.¹¹ This differ-

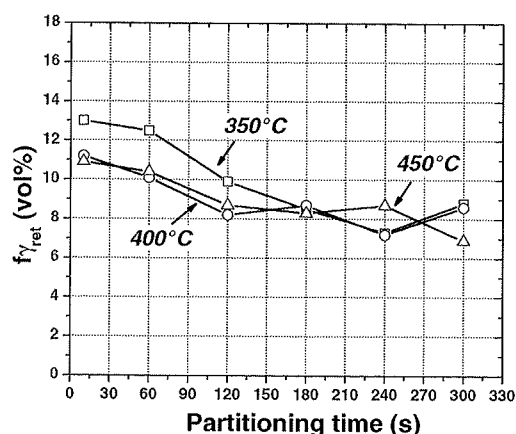


FIG. 1. Retained austenite volume fractions obtained after Q&P heat treating for the indicated partitioning temperatures applied. The experimental scatter amounts to 0.2 vol % or less.

ence may relate to sample preparation where polishing of the XRD samples may have resulted in transformation of the austenite to martensite, the fact that magnetic measurements analyze the bulk of the material whereas XRD has a limited depth of analysis, and the accuracy of correcting for texture effects by using the direct comparison method. DSC was carried out using a Netzsch 4040C apparatus. Calibration was performed by measuring the well-established melting points of high-purity indium, tin, zinc, gold, and nickel. Pt pans with an Al_2O_3 layer were used. To prevent oxidation, He gas was used at a flow rate of 50 ml/min. An empty pan was used as a reference. The baseline was determined by running the same program with two empty crucibles. Samples were cut from the heat-treated coupons using a water-cooled low speed cut-off wheel Accutom 20. The mass of the DSC specimens varied between 20 and 70 mg. The retained austenite volume fractions obtained by magnetic saturation are given in Fig. 1 for the investigated partitioning times and temperatures. Significant austenite fractions were observed; the highest volume fraction was obtained after partitioning at 350 °C for 10 s. Only a limited effect of partitioning temperature is observed for this steel. Prolonged holding at the partitioning temperature results in decreasing austenite fractions for all temperatures applied.

The thermal stability of the austenite during partitioning is clearly of importance for austenite stabilization via Q&P. In order to study this stability, the sample containing the greatest retained austenite fraction, i.e., the sample partitioned at 350 °C for 10 s was loaded in the DSC apparatus where it was heated to 600 °C at a constant rate of 15 °C/min. The resulting heat flow as a function of temperature is shown in Fig. 2. Two distinct exothermic peaks are observed. A rerun of the sample after it cooled down to room temperature (dashed line in Fig. 2) did not show any pronounced peaks.

In order to help identify the mechanism associated with these two events, a Kissinger-type kinetic analysis^{12,13} was applied, enabling determination of the activation energy based on the equation $\ln \frac{T_f^2}{\phi} = \frac{E}{RT_f} + \ln \left(\frac{E}{R} \right) - \ln(A)$, where E is the activation energy, A is the pre-exponential factor, T_f is

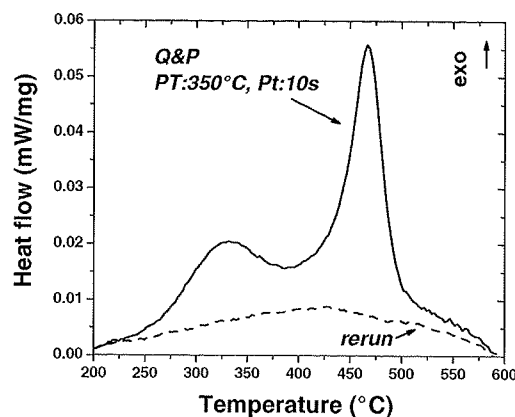


FIG. 2. DSC heat flow as a function of temperature obtained after heating the CMnSi Q&P steel from room temperature to 600 °C at a constant heating rate of 15 °C/min (solid line). A rerun of the sample after it cooled down to room temperature is also given (dashed line). Exothermic heat flow is indicated.

the peak temperature^{7,12} corresponding to a certain fraction (f') of the transformation (or other applicable process), and ϕ is the heating rate. Constant heating rates of 5, 10, 15, and 20 °C/min were applied and the resulting activation energies are given in Table I. An activation energy of 92 kJ/mol is obtained for the first event whereas a much higher activation energy of 172 kJ/mol is obtained for the second event. Owen reports an activation energy for the second stage of tempering, i.e., the decomposition of austenite in CMnSi compositions of 174 kJ/mol (Ref. 14) and proposes that this mechanism is controlled by carbon diffusion in austenite. This comparison suggests that the second exothermic peak observed in Fig. 2 is associated with austenite decomposition.

The mechanism associated with the first peak is not obvious, however, based on previous literature. In order to investigate whether the first peak can be related to (transition) carbide formation or another tempering reaction, a comparison was made between the measured activation energy and the activation energies reported for “classical” martensite tempering reactions such as carbon segregation and clustering, transition carbide and cementite formation (Table II).

Carbon segregation and carbon clustering are reported to have an activation energy of 67–91 kJ/mol (Ref. 15) as obtained by a strain aging analysis employing the model of Harper¹⁶ and Hartley,¹⁷ or 81–94 kJ/mol, as obtained from a DSC study.⁷ These values are similar to the activation energy for carbon diffusion in a bcc iron lattice i.e., 84 kJ/mol.¹⁸ Although the activation energies reported for carbon clustering are similar to the activation energy obtained for the first

TABLE I. Activation energies in kilojoule per mole associated with the observed exothermic DSC peaks.

	Peak 1	Peak 2
Q&P 350 °C 10 s	92	172
WQ		170

TABLE II. Reported activation energies in kilojoule per mole for tempering stages, bainite formation, and element diffusion.

		<i>E</i> (kJ/mol)	Ref.
Tempering stages	C clustering	67–91	15
		81–94	7
	ϵ/η formation	102–135	7
		111–118	7
		127	19
	γ_{ret} decomposition	174	14
		202	19
	Cementite formation	233	19
		227	14
Bainite formation		45	21
		49	22
		43	23
Diffusion in bcc Fe	Fe pipe diffusion	152	20
	C	84	18

peak in the Q&P sample run, carbon clustering cannot explain the exothermic event which takes place at much higher temperatures than reported for carbon clustering, reported to be completed at about 120 °C under these heating rate conditions.⁷

Another martensite tempering reaction is transition carbide formation reported to have activation energies ranging from 111 to 118 kJ/mol obtained from DSC studies⁷ or 102–135 kJ/mol according to a dilatometry study⁷ in Fe-0.97C and Fe-1.01C-1.36Cr alloys. An activation energy of 127 kJ/mol was obtained for transition carbide formation in the current alloy in a fully austenitized and water-quenched sample.¹⁹ These activation energies are intermediate between those for diffusion of carbon in bcc iron and for diffusion of iron along dislocations, so-called pipe diffusion [152 kJ/mol (Ref. 20)]. An activation energy of 227–233 kJ/mol (Refs. 14 and 19) has been reported for cementite precipitation in Si-alloyed martensitic steels.

Overall, the kinetic analysis indicates that the first calorimetric event in the Q&P sample is not associated with a “classical” tempering reaction. This conclusion is further confirmed when comparing the DSC run of the Q&P sample with a DSC run of a fully austenitized and WQ sample of the same composition as shown in Fig. 3. A constant heating rate of 15 °C/min was used in both cases. The DSC signal obtained for the WQ sample shows one exothermic peak occurring in a similar temperature range as the second event observed for the Q&P sample. An activation energy of 202 kJ/mol was obtained for the peak in the WQ sample suggesting austenite decomposition.¹⁹ A significant exothermic peak is not observed for the WQ sample in the temperature range where the first peak was observed for the Q&P sample.

The activation energy of 92 kJ/mol associated with the first DSC peak suggests a mechanism controlled by carbon diffusion in martensite, since a value of 84 kJ/mol has been reported for carbon diffusion in a bcc iron lattice.¹⁸ It is hypothesized that a plausible mechanism may be carbon par-

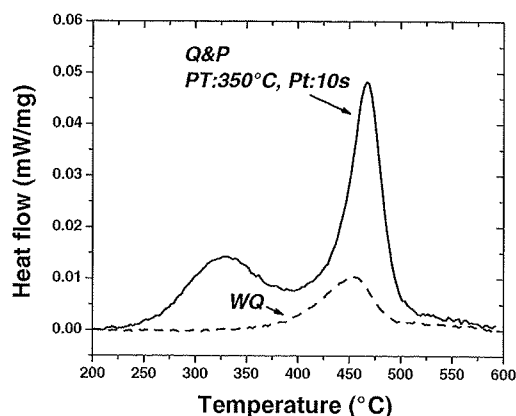


FIG. 3. Comparison of DSC signals from heating a Q&P (PT: 350 °C, Pt: 10 s) and a WQ sample at a constant rate of 15 °C/min.

tititioning from martensite into austenite. This hypothesis implies that the austenite carbon content should increase during the event of interest. In order to test this hypothesis, changes in the retained austenite fraction and carbon content were determined for conditions simulating the two DSC peak processes. In this simulation, heat treatment was performed in an air furnace using the same heating rate of 15 °C/min, followed by quenching and subsequent x-ray analysis. Q&P samples (PT: 350 °C, Pt: 10 s) were heated from room temperature to 400 °C (beyond the first peak) or to 575 °C (beyond the second peak). The austenite fractions and carbon concentrations as measured via XRD are given in Table III. Heating to 400 °C results in an increase in austenite carbon content without a substantial change in retained austenite volume fraction. Thus, it appears that the first DSC peak is related to carbon partitioning from martensite into austenite with kinetics controlled by carbon diffusion in the bcc phase. Since the retained austenite fraction obtained after heating to 400 °C is similar to the fraction before heating, the peak is not believed to be related to bainite formation. The reported activation energy for bainite formation [43–49 kJ/mol (Refs. 21–23)] is also inconsistent with the DSC results.

Heating to 575 °C results in a significant reduction in the retained austenite fraction and a decrease in austenite carbon content. This behavior confirms that the second event is associated with austenite decomposition, likely into a ferrite/carbide mixture.

THERMO-CALC® software was used to estimate the enthalpy change associated with the measured carbon increase

TABLE III. Retained austenite fraction (vol %) and carbon content (wt %) of Q&P samples: as heat treated (PT: 350 °C, Pt: 10 s), reheated to 400 °C or 575 °C at 15 °C/min.

Condition	$f_{\gamma_{\text{ret}}}$, XRD (vol %)	C content (wt %)
As heat treated	6.2 ± 0.5	1.17 ± 0.01
400 °C	5.7 ± 0.3	1.53 ± 0.02
575 °C	2.3 ± 0.4	0.97 ± 0.02

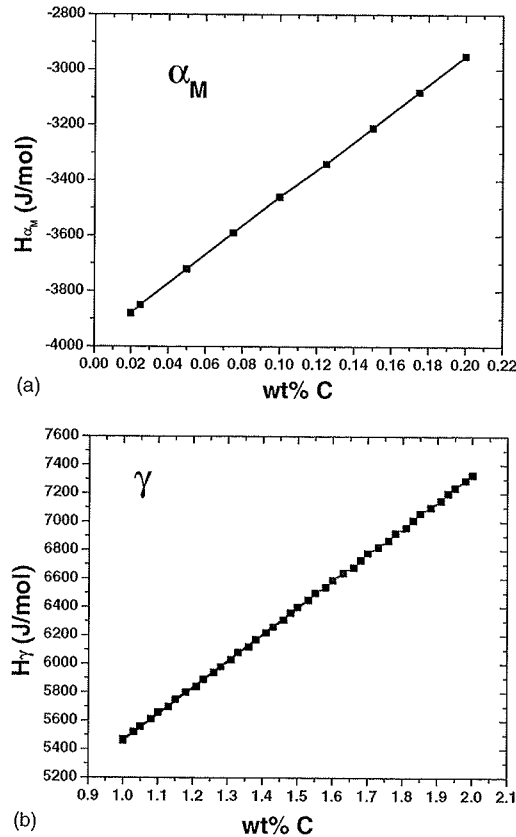


FIG. 4. Molar enthalpy (J/mol) calculated using THERMO-CALC for a Fe-C-1.63Mn-1.63Si composition as a function of carbon content (wt %) in (a) supersaturated ferrite for a carbon content ranging from 0.02 to 0.2 wt % and (b) austenite for a carbon content ranging from 1.0 to 2.0 wt %.

in the austenite (Table III) and corresponding carbon decrease in the martensite when heating the sample to 400 °C, assuming that the first DSC peak is associated with the hypothesized carbon partitioning mechanism. The calculated molar enthalpy change as a function of carbon content for supersaturated ferrite and austenite using the TCFE database is given in Fig. 4. The retained austenite volume fraction was assumed to remain constant in the calculations and carbide precipitation was not considered. The molar-enthalpy change ($\Delta\bar{H}$) associated with a carbon increase in the austenite (γ) and corresponding decrease in the ferrite (α_M) was calculated according to $\Delta\bar{H} = \bar{H}_{final} - \bar{H}_{initial}$
$$= \frac{(\text{mol } \alpha_M \bar{H}_{\alpha_M} + \text{mol } \gamma \bar{H}_{\gamma})_{final} - (\text{mol } \alpha_M \bar{H}_{\alpha_M} + \text{mol } \gamma \bar{H}_{\gamma})_{initial}}{\text{mol alloy}}$$
 with \bar{H} the molar enthalpy, and final and initial conditions referring to the carbon contents in the as heat-treated (Q&P) state, i.e., 1.17 wt % assumed to be homogenous throughout the 6.2 vol % austenite and a carbon content after heating the sample to 400 °C as indicated in Table III, respectively. A

value of -60 J/mol was obtained. The measured enthalpy release for reheating the sample to 400 °C obtained from the surface under the DSC heat-flow curve as a function of temperature (Fig. 2) amounts to -76 J/mol. Note that the rerun (dotted line in Fig. 2) was subtracted from the curve for the calculation to correct the background. Values of a similar order of magnitude are obtained suggesting that the first peak is related to the thermal signature of carbon partitioning from martensite into austenite.

It should be noted that diffusion calculations using DICRTA® predict very fast partitioning kinetics on the order of a second or less to obtain full decarburization of the martensite.^{24,25} This would imply that full decarburization of the martensite should already have been completed in the Q&P sample partitioned at 350 °C for 10 s. Atom probe tomography, however, indicated that about 0.1 wt % carbon was present in the martensite of a Q&P heat-treated sample (PT=350 °C, Pt=10 s) of similar alloy composition.⁵ This suggests that carbon depletion may be slower than predicted by DICRTA. It should be recognized that the model calculations assume carbon supersaturated ferrite instead of a martensitic microstructure and potential effects of dislocations and their associated strain field for interstitials on carbon diffusion are not incorporated. It is worthwhile mentioning that diffusivity of hydrogen decreases with increased degree of cold working which is attributed to an increased dislocation density.²⁶ It can also be noted that the strength levels reported after these short partitioning treatments³ may not be obtained in microstructures where the martensite is fully carbon depleted.

In conclusion, DSC was employed to study Q&P microstructures primarily consisting of martensite and retained austenite. A Q&P heat-treated sample partitioned at a relatively low temperature of 350 °C for a relatively short time of 10 s was loaded into the DSC apparatus and heated to 600 °C. Two exothermic events were observed. An activation energy close to the activation energy for carbon diffusion in ferrite was obtained for the first event and an increase in the austenite carbon content was confirmed to be associated with this peak. The measured signal could not be explained by “classical” tempering reactions such as (transition) carbide formation. The enthalpy change associated with carbon partitioning from martensite into austenite as computed using THERMO-CALC was similar to the enthalpy associated with the integrated DSC peak. The second DSC peak was related to austenite decomposition, based on XRD measurements and comparison of the measured activation energy with literature values.

This research was funded by the Institute for the Promotion of Innovation through Science and Technology in Flanders (IWT-Vlaanderen). The support of the sponsors of the Advanced Steel Processing and Products Research Center, an industry/university cooperative research center at the Colorado School of Mines is gratefully acknowledged.

- ¹J. G. Speer, D. K. Matlock, B. C. De Cooman, and J. G. Schroth, *Acta Mater.* **51**, 2611 (2003).
- ²E. De Moor, S. Lacroix, A. J. Clarke, J. Penning, and J. G. Speer, *Metall. Mater. Trans. A* **39**, 2586 (2008).
- ³H. Y. Li, X. W. Lu, W. J. Li, and X. J. Jin, *Metall. Mater. Trans. A* **41**, 1284 (2010).
- ⁴M. J. Santofimia, L. Zhao, and J. Sietsma, *Metall. Mater. Trans. A* **40**, 46 (2009).
- ⁵A. J. Clarke, J. G. Speer, M. K. Miller, R. E. Hackenberg, D. V. Edmonds, D. K. Matlock, F. C. Rizzo, K. D. Clarke, and E. De Moor, *Acta Mater.* **56**, 16 (2008).
- ⁶M. J. Van Genderen, M. Isac, A. Böttger, and E. J. Mittemeijer, *Metall. Mater. Trans. A* **28**, 545 (1997).
- ⁷P. V. Morra, A. J. Böttger, and E. J. Mittemeijer, *J. Therm. Anal. Calorim.* **64**, 905 (2001).
- ⁸A. Clarke, J. G. Speer, D. K. Matlock, F. C. Rizzo, D. V. Edmonds, and K. He, *Solid-Solid Phase Transformations in Inorganic Materials* (TMS, Warrendale, PA, 2005).
- ⁹L. Zhao, N. H. Van Dijk, E. Brück, J. Sietsma, and S. van der Zwaag, *Mater. Sci. Eng., A* **313**, 145 (2001).
- ¹⁰B. D. Cullity, *Stock SR Elements of X-Ray Diffraction* (Prentice-Hall, New York, 2001).
- ¹¹P. J. Jacques, S. Allain, O. Bouaziz, A. De, A.-F. Gourgues, B. M. Hance, Y. Houbaert, J. Huang, A. Iza-Mendia, S. E. Kruger, M. Radu, L. Samek, J. Speer, L. Zhao, and S. van der Zwaag, *Mater. Sci. Technol.* **25**, 567 (2009).
- ¹²U. K. Viswanathan, T. R. G. Kutty, and C. Ganguly, *Metall. Mater. Trans. A* **24**, 2653 (1993).
- ¹³E. J. Mittemeijer, *J. Mater. Sci.* **27**, 3977 (1992).
- ¹⁴W. S. Owen, *Trans. Am. Soc. Met.* **46**, 812 (1954).
- ¹⁵A. K. De, S. Vandeputte, and B. C. De Cooman, *J. Mater. Eng. Perform.* **10**, 567 (2001).
- ¹⁶S. Harper, *Phys. Rev.* **83**, 709 (1951).
- ¹⁷S. Hartley, *Acta Metall.* **14**, 1237 (1966).
- ¹⁸C. A. Wert and R. M. Thomson, *Physics of Solids* (McGraw-Hill, New York, 1964).
- ¹⁹E. De Moor, S. Lacroix, L. Samek, J. Penning, and J. G. Speer, in *Proceedings of the Third International Conference on Advanced Structural Steels*, 2006 (The Korean Institute of Metals and Materials, Seoul, Korea, 2006), p. 873.
- ²⁰M. Cohen, *Trans. Jpn. Inst. Met.* **11**, 145 (1970).
- ²¹N. V. Luzginova, L. Zhao, and J. Sietsma, *Mater. Sci. Eng., A* **481-482**, 766 (2008).
- ²²M. Umemoto, K. Horiuchi, and I. Tamura, *Trans. Iron Steel Inst. Jpn.* **22**, 854 (1982).
- ²³S. M. C. van Bohemen, M. J. Santofimia, and J. Sietsma, *Scr. Mater.* **58**, 488 (2008).
- ²⁴M. J. Santofimia, J. G. Speer, A. J. Clarke, L. Zhao, and J. Sietsma, *Acta Mater.* **57**, 4548 (2009).
- ²⁵A. J. Clarke, J. G. Speer, D. K. Matlock, F. C. Rizzo, D. V. Edmonds, and M. J. Santofimia, *Scr. Mater.* **61**, 149 (2009).
- ²⁶W. Y. Choo and J. Y. Lee, *Metall. Mater. Trans. A* **14**, 1299 (1983).